Tip-Enhanced Raman Scattering: Approaching 10 nm Optical Resolution

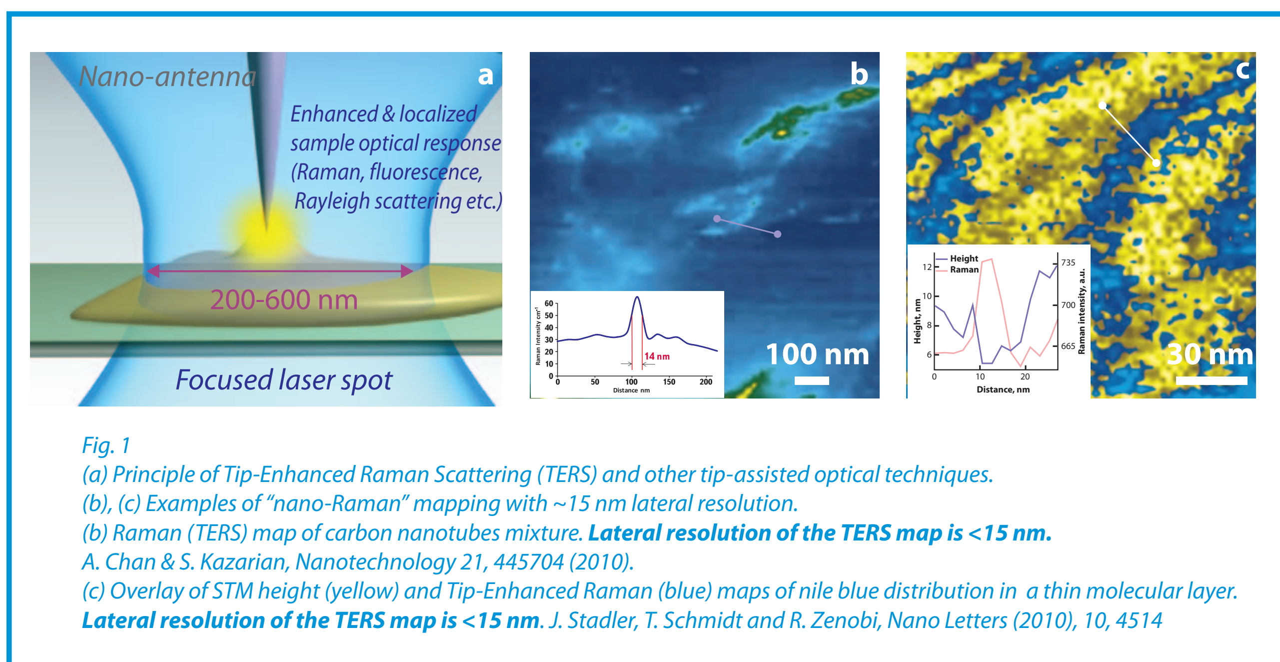

Fig. 1
(a) Principle of Tip-Enhanced Raman Scattering (TERS) and other tip-assisted optical techniques.
(b), (c) Examples of "nano-Raman" mapping with ~15 nm lateral resolution.
(b) Raman (TERS) map of carbon nanotubes mixture. ***Lateral resolution of the TERS map is <15 nm.***
A. Chan & S. Kazarian, Nanotechnology 21, 445704 (2010).
(c) Overlay of STM height (yellow) and Tip-Enhanced Raman (blue) maps of nile blue distribution in a thin molecular layer.
Lateral resolution of the TERS map is <15 nm*. J. Stadler, T. Schmidt and R. Zenobi, Nano Letters (2010), 10, 4514*

The resolution of "classical" optical imaging is limited by diffraction. Light cannot be focused by conventional refractive or reflection optics into a spot smaller than half of the wavelength (about 200 nm for visible light). This fact has a lower size limit on light microscopy and spectroscopy for the last few centuries. Currently, new optical microscopy techniques are being developed that break the Abbe diffraction limit and give the capability to resolve features smaller than 100 nm by using visible light.

HIGH RESOLUTION OPTICAL IMAGING BY TIP-ASSISTED TECHNIQUES

One of the promising approaches that break the optical diffraction limit is the so-called "apertureless" or "tip assisted" technique. A nano-antenna (specially prepared AFM probe) is excited by a tightly focused excitation laser spot (Fig. 1 (a)), placed at the apex or depending on nano-antenna working principle, at some other part of nano-antenna. Under specific conditions, the nano-antenna can localize and enhance the excitation electromagnetic field and/or sample optical response in very close proximity of the tip apex. The nano-antenna apex effectively works as a localized "nano-emitter" or "nano-scatterer" of light. When scanning the sample with respect to such a nano-antenna, the obtained map of sample optical response (Raman and Rayleigh scattering,

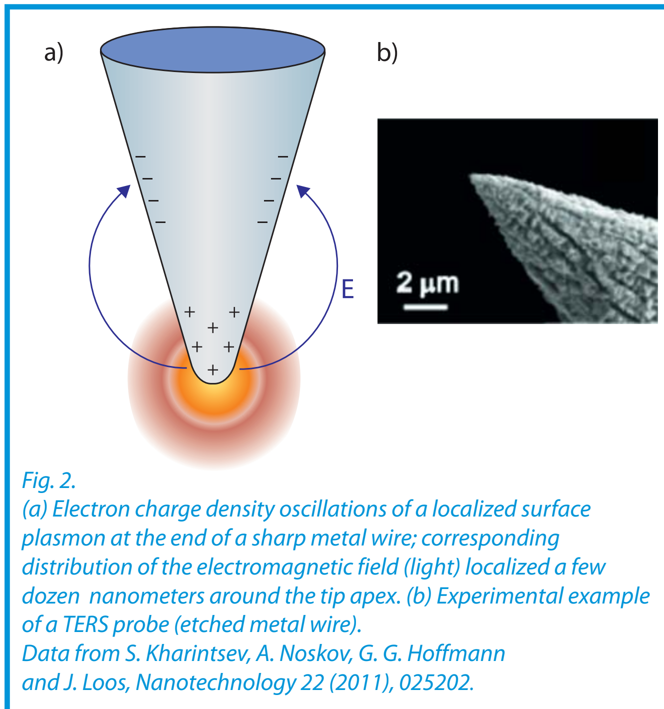

Fig. 2.
(a) Electron charge density oscillations of a localized surface plasmon at the end of a sharp metal wire; corresponding distribution of the electromagnetic field (light) localized a few dozen nanometers around the tip apex. (b) Experimental example of a TERS probe (etched metal wire).
Data from S. Kharintsev, A. Noskov, G. G. Hoffmann and J. Loos, Nanotechnology 22 (2011), 025202.

fluorescence, etc.) has a lateral resolution which is determined not by the laser spot size but by the size of electromagnetic field localization at the nano-antenna apex.
Theoretically, the resolution of such tip-assisted techniques can reach size scales less than 10 nm, leading to true nanoscale optical imaging.
One of the most common type of tip-assisted optical imaging techniques is Tip-Enhanced Raman Scattering (TERS or “nano-Raman”)– when a nano -antenna is used to locally enhance the Raman scattering signal from a sample. Raman maps with nanometer scale resolution provide a route for chemical identification on the nanometer scale.
Fig. 1 (b), (c) show examples of “nano-Raman” maps of various objects with a resolution of ~12–15 nm which is – close to the theoretical limit.
There also exist other tip-assisted techniques for high resolution optical microscopy: Tip Enhanced Fluorescence Microscopy, TEFM (when a sample’s fluorescence signal is enhanced); scattering near-field optical microscopy, s-SNOM (when light elastically scattered by a nano-antenna is measured) and others. In the remainder of this paper we will mainly use the “TERS” acronym to describe the experiments, instrumentation and measurements procedures since TERS experiments are the most widely used. TEFM and s-SNOM experiments are essentially the same as TERS from hardware point of view. They only differ in types of probes used, and the optical signal measured.

NANO-ANTENANS FOR TERS AND OTHER TIP-ASSISTED OPTICAL TECHNIQUES

The commonly used type of a nano-antenna for nano-scale optical imaging is a sharp metal tip (usually gold or silver) which has a localized surface plasmon at the very end (Fig. 2(a)) having a frequency close to that of the excitation laser light. The power density of the light can be locally increased by many orders of magnitude in the area within 10–50 nm of the tip end. Tips are usually either etched from a metal wire (Fig. 2 (b)) or metal is deposited onto a standard AFM cantilever.
Several, more elaborate probes are also used as nano-antennas: metal tips with bow-tie structures at the end, tips with special periodic structures for effective excitation and focusing of surface plasmon polaritons and some others.

PRINCIPALS BEHIND THE SUCCESSFUL TERS EXPERIMENT

In order to study the interaction between light and an AFM probe (nano-antenna), the following strict requirements are necessary for the instrumentation:
Integration of the AFM with high resolution objective lenses in different configurations (Fig. 3)
Illumination and signal collection from the top, from the bottom, and from the side is required for different experiments and different sample types. A high resolution (high numerical aperture - NA) objective lens is the key factor for the successful measurement of TERS signals. It maximizes light collection efficiency and, at the

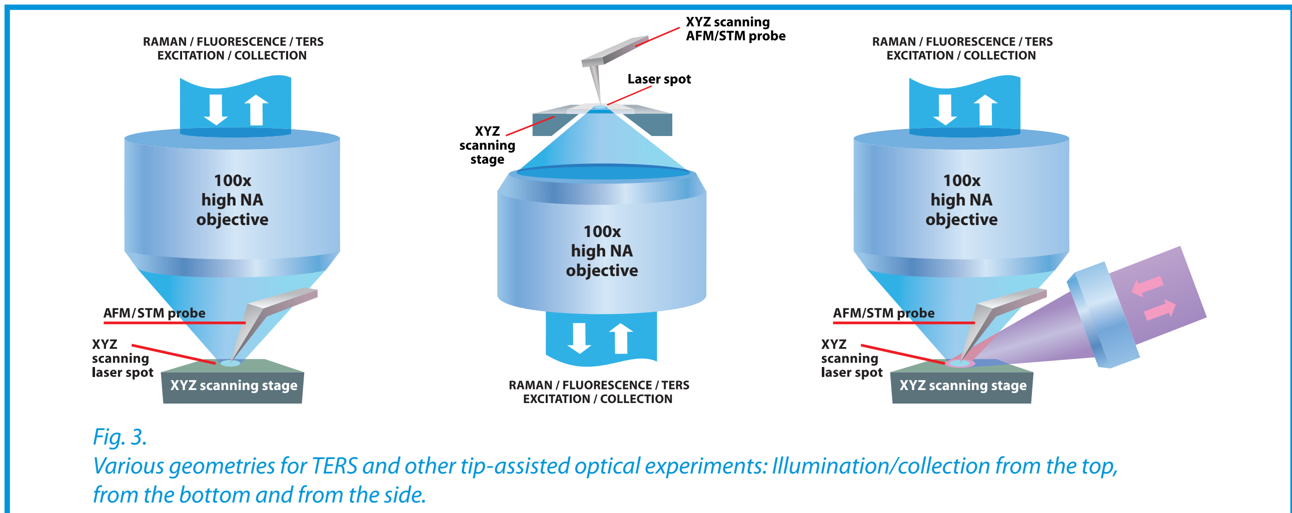

Fig. 3.
Various geometries for TERS and other tip-assisted optical experiments: Illumination/collection from the top, from the bottom and from the side.

same time, minimizes collateral excitation and collection of the non-enhanced optical signal coming from the sample.

Dual Scan: sample scanning AND laser spot scanning relative to AFM probe

For successful TERS mapping not only should the sample be scanned with nanometer precision but also the AFM probe must be positioned automatically inside the laser spot with the precision of a few tens of nm. To accomplish this task, the tightly focused laser spot or the tip should be automatically scanned with respect to one another in the X,Y and Z directions with nm accuracy and repeatability.

Ability to support different AFM probes: AFM cantilevers, STM tips, different etched wires, etc.

There are many different types of nano-antennas. In order to be able to work with all of them, the instrument must support many possible types of AFM probes (cantilevers, wires, fibers, etc.) and all types of feedback mechanisms (laser feedback, tuning fork feedback, tunneling current feedback).

Mechanical stability

In order to detect the near-field effects that produce high resolution optical maps, a nano-antenna has to be positioned a few nm from the sample and it's proximity maintained with very high stability without damaging the sensitive TERS tip. This dictates requirements for precision, speed and sensitivity of the AFM feedback electronics and mechanical stability of the system. Mechanical and temporal stability is also crucial in keeping the nano-antenna precisely inside tightly focused laser spot for long-term experiments.

Integration with a dedicated Raman spectrometer

The key requirements for a well integrated Raman system for TERS experiment are: properly expanded and collimated excitation laser beam to achieve the minimum laser spot size on the sample; high confocality for minimizing "background" (non-enhanced) signal detected from the sample; fast automated changing of the excitation lasers and automated polarization rotation for optimizing the resonant excitation of surface plasmons in the nano-antenna; high sensitivity and imaging speed.

Seamless software and hardware integration of AFM and optical spectroscopy techniques

Unified and comprehensive control software is required to run a complicated TERS experiment combining all of the AFM and spectroscopy hardware capabilities. All Raman and AFM components of the instrument should be easily controlled from the same program. The software should not be a limiting factor for the TERS scanning speed- all delays when communicating with scanners and optical detectors should be minimized. AFM, Raman and TERS images should be collected and analyzed in one seamless software program.

All of the above requirements are successfully realized in the NTEGRA Spectra AFM-Raman-SNOM-TERS instrument (http://www.ntmdt.com/device/ntegra-spectra). TERS data obtained on the NTEGRA Spectra are shown below.

Graphene imaged by nano-Raman (TERS)

Using a Silver STM tip as a TERS probe

Fig. 4 (a) shows TERS image of graphene (produced by standard CVD on a copper substrate) obtained by using etched silver STM tip as a TERS probe. The experiment is done in the so-called "gap-mode": when both tip and substrate are metallic and tunneling current feedback is used.

The green color represents intensity of the graphene 2D band – corresponding to pristine graphene areas. The blue color shows intensity in the 2800–3000 cm^{-1} region (typical for CH stretching modes) – corresponding to areas with CH-terminated graphene. It is notable that CH stretching bands are not seen at all in conventional confocal Raman images – due to their very low intensity. TERS image of graphene produced by the Scotch-tape method and deposited onto a gold substrate is shown on Fig. 4 (b). Two defect areas inside the single graphene layer are identified on the image by the intensity of D-band (red areas, marked by solid line circles). The dimensions of the defect areas are 75x45 nm^2 and 55x25 nm^2 respectively. Precise analysis of line cross-sections taken from the above Raman maps shows that all the TERS images were recorded with *lateral resolution less than 12 nm.*

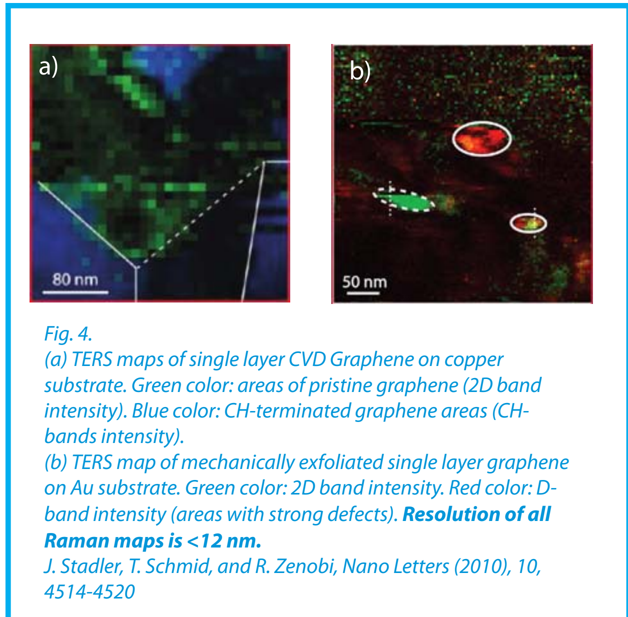

Fig. 4.
(a) TERS maps of single layer CVD Graphene on copper substrate. Green color: areas of pristine graphene (2D band intensity). Blue color: CH-terminated graphene areas (CH-bands intensity).
(b) TERS map of mechanically exfoliated single layer graphene on Au substrate. Green color: 2D band intensity. Red color: D-band intensity (areas with strong defects). ***Resolution of all Raman maps is <12 nm.***
J. Stadler, T. Schmid, and R. Zenobi, Nano Letters (2010), 10, 4514-4520

Using a Gold Coated Cantilever

Fig. 5 shows TERS data on multi-layer graphene (on Si/SiO_2 substrate) using an Au-coated cantilever as a TERS probe. The TERS enhancement takes place only when the localized surface plasmon at the tip has energy close to that of the excitation laser photons. This is clearly demonstrated in Fig. 5 (a) showing experimental wavelength dependence of the enhancement. TERS spectra are given for red, green and blue excitation lasers and compared to conventional confocal Raman spectrum taken away from the TERS probe. The TERS enhancement factor reaches its maximum for the green laser.

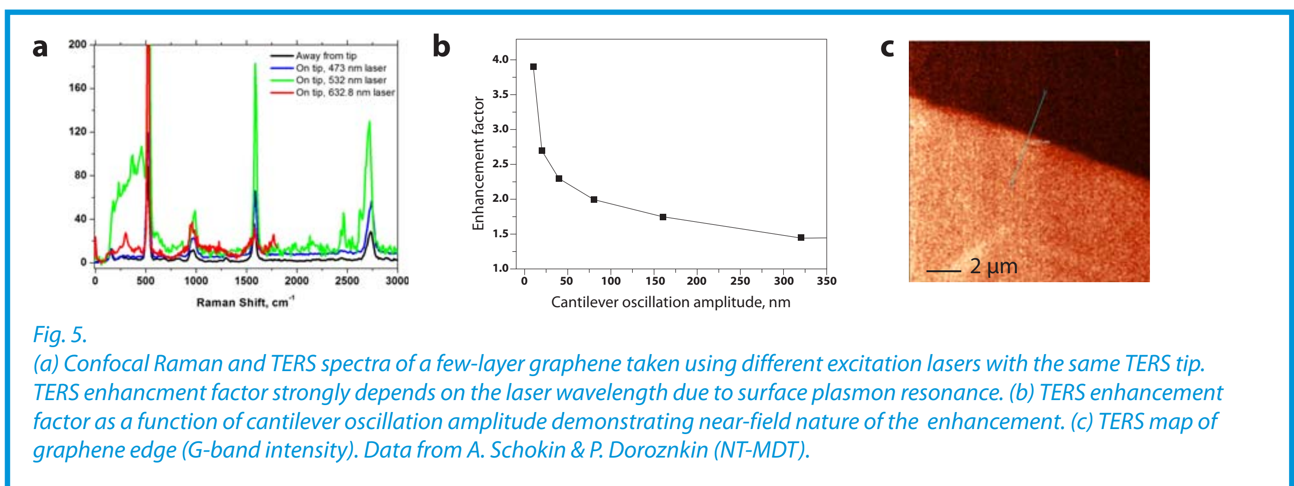

Fig. 5.
(a) Confocal Raman and TERS spectra of a few-layer graphene taken using different excitation lasers with the same TERS tip. TERS enhancment factor strongly depends on the laser wavelength due to surface plasmon resonance. (b) TERS enhancement factor as a function of cantilever oscillation amplitude demonstrating near-field nature of the enhancement. (c) TERS map of graphene edge (G-band intensity). Data from A. Schokin & P. Doroznkin (NT-MDT).

Fig. 5 (b) shows TERS enhancement factor as a function of cantilever oscillation amplitude. It rapidly increases for cantilever amplitudes smaller than 50 nm, demonstrating the spatial localization of the TERS enhancement effect. The TERS map (intensity of the G-band) of the graphene edge area is given in Fig. 5 (c), showing lateral resolution much higher than conventional confocal Raman microscopy.

Silicon-based Structures Imaged by TERS

Imaging and Strain Analysis of Nano-scale SiGe Semiconductor Structures

The periodic SiGe line structure, Fig. 6 (a), is used as a test sample for TERS imaging of nanoscale Si devices – to study chemical composition and crystal lattice stress. The line structure has an average period of 95 nm – comparable to the dimensions encountered in presently available CMOS devices.

Simultaneously measured AFM and TERS maps are shown in Fig. 6 (c), (d), (e). The periodic line structure is clearly resolved in the Raman images, indicating the lateral resolution of the Raman maps. As seen in the line profile, the intensity of the Raman signal from the SiGe layer, (Fig. 6 (e)), increases sharply at the position of each SiGe line due the higher SiGe thickness (40 nm) compared to 10 nm thickness between the lines. Conversely, the Raman signal from the Si substrate is diminished at the positions of each SiGe line. Because the enhancing TERS tip in these areas is far away (>50 nm) from the substrate the TERS enhancement from the Si disappears.

Fig. 6 (b) compares Raman spectra taken from the individual SiGe lines and from the area of a thin, 10 nm, SiGe layer away from the line structure. Raman band positions are used to calculate stress values. The obtained results show the intrinsic stress ($\sigma_{xx} = \sigma_{yy} = \sigma_0 = -1.53$ GPa) within the remnant 10 nm thick SiGe layer away from the line pattern.

The patterning process leads to strong stress relaxation within the freestanding SiGe lines. From the spectra acquired from the TERS measurements, a stress value of approximately σ_{xx} = - 190 MPa is calculated, corresponding to a stress relaxation of about 88% compared to the initial value before pattering. The relaxation of the compressive stress within the SiGe lines induces tensile stress in the substrate below the lines as shown in Fig. 6 (b). This small amount tensile stress could be the reason for the observed slight special shift of the Si substrate peak to lower wavenumbers as compared to the stress-free peak position.

The achieved results demonstrate the capability of the TERS technique to characterize the stress in Si based nanostructures with <50 nm spatial resolution – as required for the investigation of current leading edge CMOS devices.

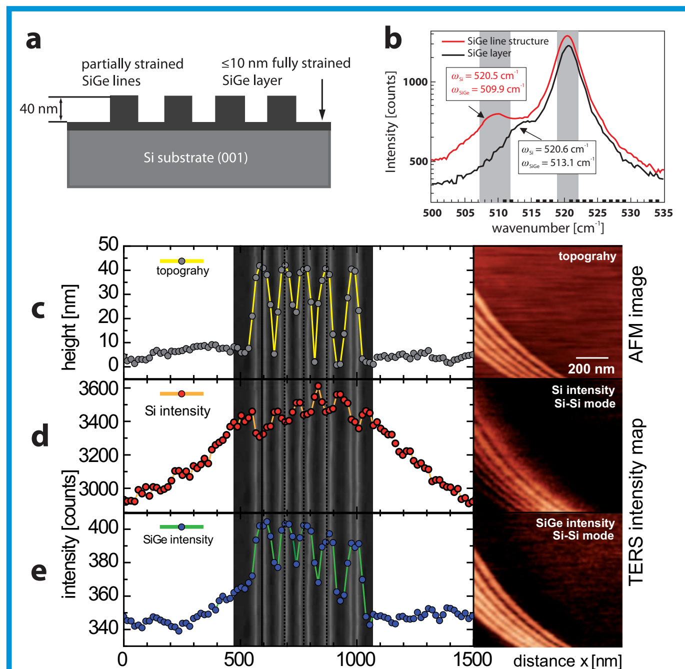

Fig.6
(a) Periodic SiGe line structure on Si substrate.
(b) Comparison of TERS spectra from a SiGe line (red) and the remnant thin SiGe area a few µm away from the line structure. Peak positions of SiGe band are different indicating different stress states. (c) AFM topography and (d), (e) simultaneously measured TERS maps of Si-Si phonon band in Si and in SiGe material correspondingly; right panels show 2D maps (2x2 µm), left panels show corresponding line cross-section (from the lowest scan line).
Resolution of Raman maps is <50 nm.
Data from P. Hermann, M. Hecker, D. Chumakov, M. Weisheit, J. Rinderknecht, A. Shelaev, P. Dorozhkin, L. M. Eng, Ultramicroscopy 111(2011) 1630-1635

Carbon Nanotubes Imaged by Nano-Raman (TERS)

Au coated AFM cantilever as a TERS probe
Conventional micro-Raman and TERS mapping of single-walled carbon nanotubes is shown in Fig. 7. Nanotubes were deposited from solution onto a microscope cover glass substrate. Experiments were done in the inverted geometry (illumination from bottom) using a 633 nm excitation laser and an Au coated cantilever as the TERS probe. The Confocal Raman map of the sample (Fig. 7(a)) has a diffraction limited resolution of 250 nm. Details of nanotube bundles are not revealed in the image. The TERS image in Fig. 7(b),(c) gives a lateral resolution of ~14 nm and provides detailed information about the structure of the nanotube aggregates. A complete Raman spectrum was recorded at every pixel of the TERS map (100x100 pixel image). Detailed analysis of different Raman bands on the obtained TERS map allowed differentiating nanotubes of different types (metallic or semiconducting), different diameters, as well as detecting nanosize amorphous carbon contaminants with a resolution close to 10 nm.

Etched Au wire as TERS probe
The TERS image of an individual single walled nanotube bundle measured with an etched metal wire as the TERS probe is shown in Fig. 8 and resolution of 50 nm is demonstrated. Fig. 8 (c) shows the tip approach curves (TERS enhancement factor as a function of tip-sample distance) for two types of TERS probes: horizontally oscillating metal wire attached to the tuning fork (oscillation amplitude <10 nm) and vertically oscillating AFM cantilever (oscillation amplitude ~40 nm). The data for the tuning fork demonstrated that TERS effect is localized to approximately 10 nm near the tip. The approach curve for the AFM cantilever is less steep due to the large amplitude of vertical oscillation. Even though average distance from the cantilever tip to the sample is large (~30 nm), during part of the oscillation cycle the tip is only a few nm from the sample, producing a visible enhancement. Measurements were performed in the inverted AFM-Raman geometry.

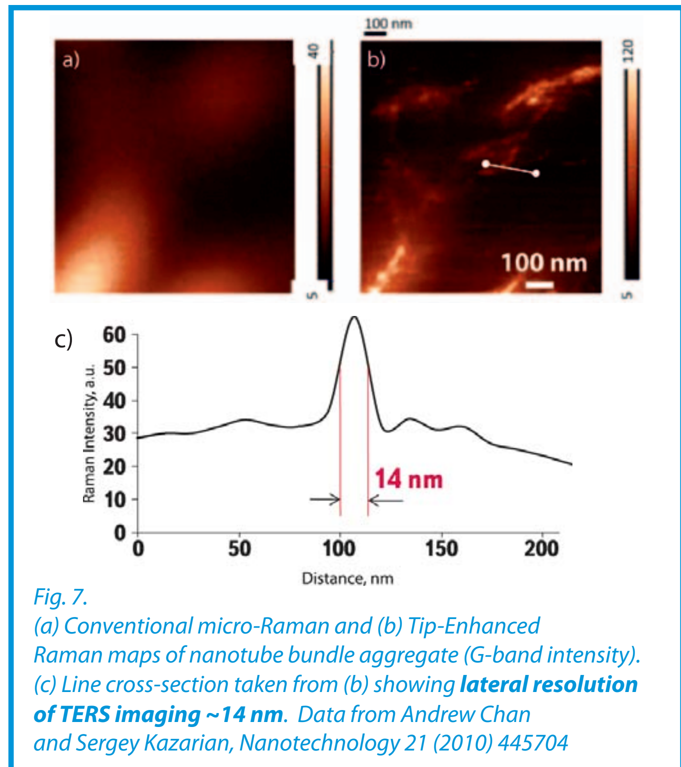

Fig. 7.
*(a) Conventional micro-Raman and (b) Tip-Enhanced Raman maps of nanotube bundle aggregate (G-band intensity). (c) Line cross-section taken from (b) showing **lateral resolution of TERS imaging ~14 nm**. Data from Andrew Chan and Sergey Kazarian, Nanotechnology 21 (2010) 445704*

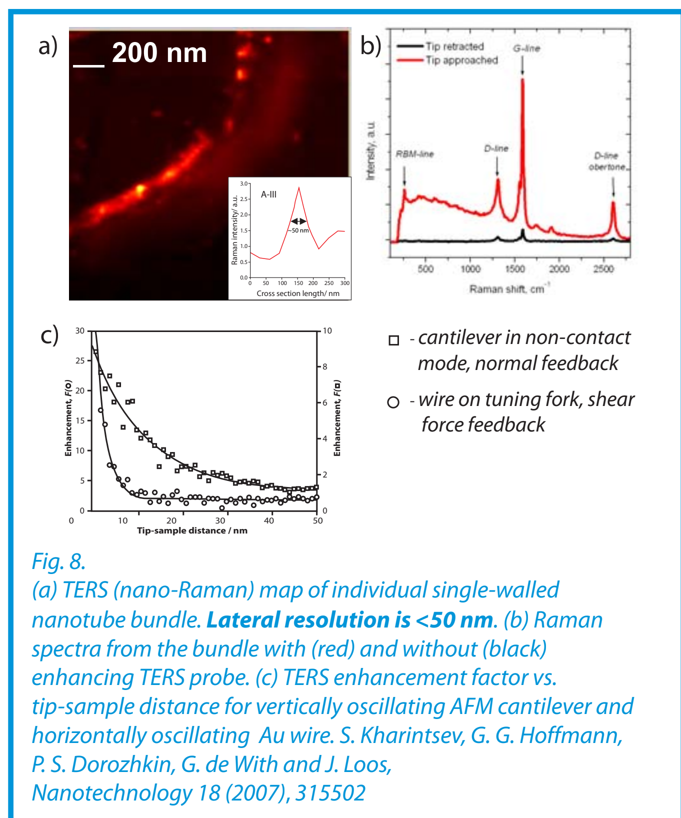

Fig. 8.
*(a) TERS (nano-Raman) map of individual single-walled nanotube bundle. **Lateral resolution is <50 nm**. (b) Raman spectra from the bundle with (red) and without (black) enhancing TERS probe. (c) TERS enhancement factor vs. tip-sample distance for vertically oscillating AFM cantilever and horizontally oscillating Au wire. S. Kharintsev, G. G. Hoffmann, P. S. Dorozhkin, G. de With and J. Loos, Nanotechnology 18 (2007), 315502*

Polymers Imaged by Nano-Raman (TERS)

Phase separation studies of polymer blend film

Phase separation behavior of a partially miscible PMMA / SAN (70 / 30 wt %) thin polymer film was studied by TERS mapping. Regular confocal Raman and TERS spectra from the film are compared on Fig. 9 (a). The spectra were recorded at the same aquisition time. The net enhancement factor of Raman signal is ~15x that corresponds to ~1500x enhancement factor when normalized to the TERS enhancement area (~20x20 nm^2). Such TERS enhancement allows mapping with much higher speed and lateral resolution compared to conventional confocal mapping. TERS maps of the SAN Raman band for the thin film after 2 min annealing at 250 °C are shown in Fig. 9 (b), (c). No sharp phase boundary is observed on Fig. 9 (c) indicating an early stage of the phase separation for the given annealing conditions. Meanwhile, films treated for 5 min at 250 °C showed completely different phase separation behavior with larger SAN domains and sharper phase boundaries.

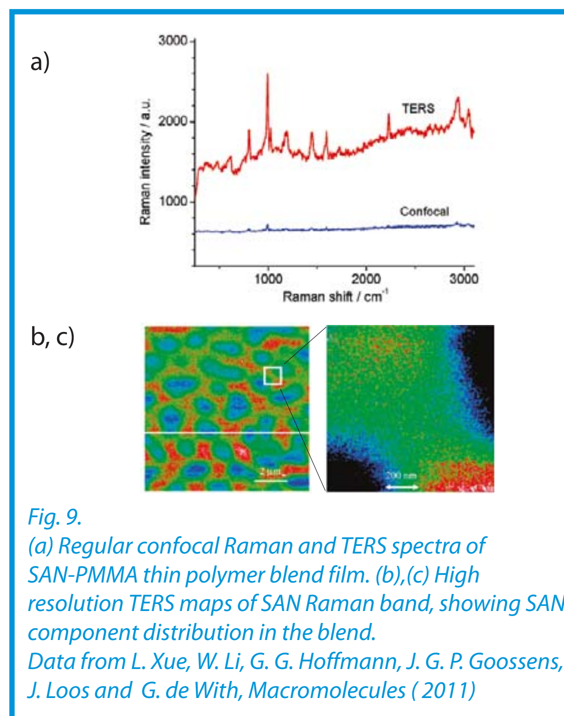

Fig. 9.
(a) Regular confocal Raman and TERS spectra of SAN-PMMA thin polymer blend film. (b),(c) High resolution TERS maps of SAN Raman band, showing SAN component distribution in the blend.
Data from L. Xue, W. Li, G. G. Hoffmann, J. G. P. Goossens, J. Loos and G. de With, Macromolecules (2011)

Organic Samples Imaged by TERS

High resulition TERS mapping of thin organic films on Au substrate

Fig. 10 (a) compares confocal Raman and TERS spectra of a thin nile blue (NB) / brilliant cresyl blue (BCB) layer on a gold substrate. An etched silver tip is used in STM feedback regime with the gap-mode geometry. The conventional confocal Raman signal from the layer is almost absent, while the TERS spectrum shows strong Raman bands specific

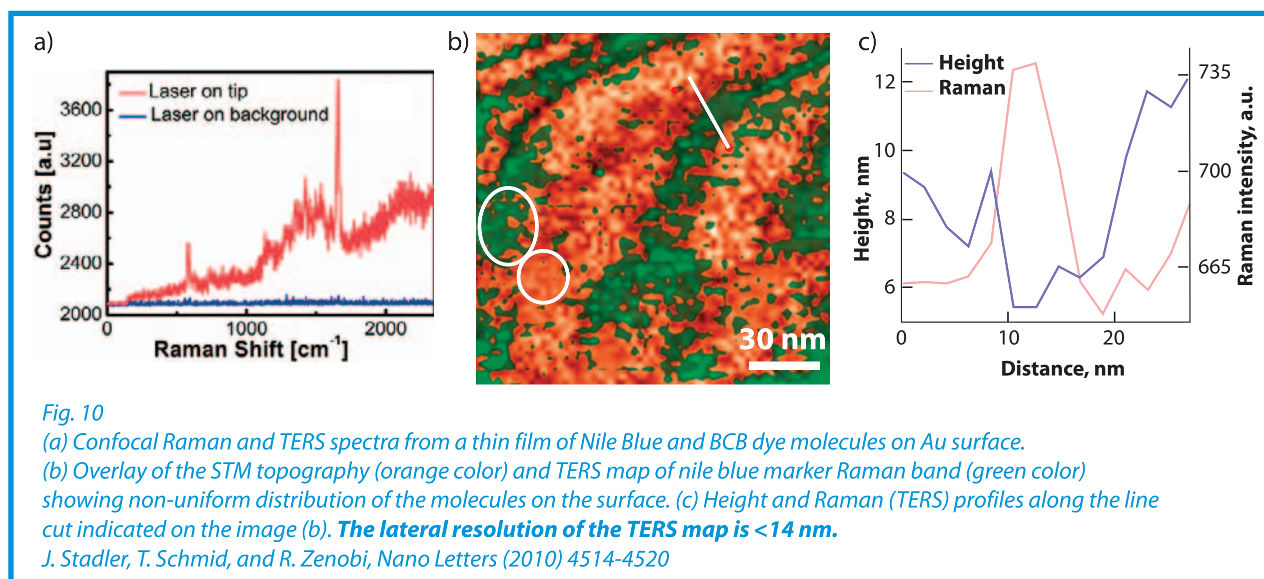

Fig. 10
(a) Confocal Raman and TERS spectra from a thin film of Nile Blue and BCB dye molecules on Au surface.
(b) Overlay of the STM topography (orange color) and TERS map of nile blue marker Raman band (green color) showing non-uniform distribution of the molecules on the surface. (c) Height and Raman (TERS) profiles along the line cut indicated on the image (b). ***The lateral resolution of the TERS map is <14 nm.***
J. Stadler, T. Schmid, and R. Zenobi, Nano Letters (2010) 4514-4520

to the NB and BCB molecules. The TERS enhancement factor is estimated to be at least 10^7 - enough for single molecular sensitivity in Raman imaging. The overlay of the STM and TERS (NB band intensity) images shown on Fig. 10 (b) demonstrates non-uniform distribution of the molecules on the substrate. In some areas the density of NB molecules is correlated with the topography of the surface; in other areas (example shown by circles), non-uniform distribution of molecules is observed on completely flat areas of the substrate. The selected line profile of Raman intensity from the TERS map Fig. 10 (c) shows the resolution of Raman imaging to be at least 14 nm.

TERS imaging of patterned thiol monolayers

Distribution of two isomeric thiols (2-mercaptopyridine (2-PySH) and 4-mercaptopyridine (4-PySH)) in a self-assembled monolayer (SAM) on a gold surface was measured by STM-TERS (Fig. 11). The circle pattern of the 2-PySH thiol SAM was produced by micro-contact printing. SAMs of such thiols are used as protective layers on metal surfaces, act as a basis for (bio-)sensors, and have been proposed as components for molecular electronics. The large signal enhancement of TERS was employed here to detect monolayer coverage of weakly scattering analytes that are not detectable with normal Raman spectroscopy. This emphasizes the usefulness of TERS for studies of organic samples that are not at feasible by conventional Raman spectroscopy.

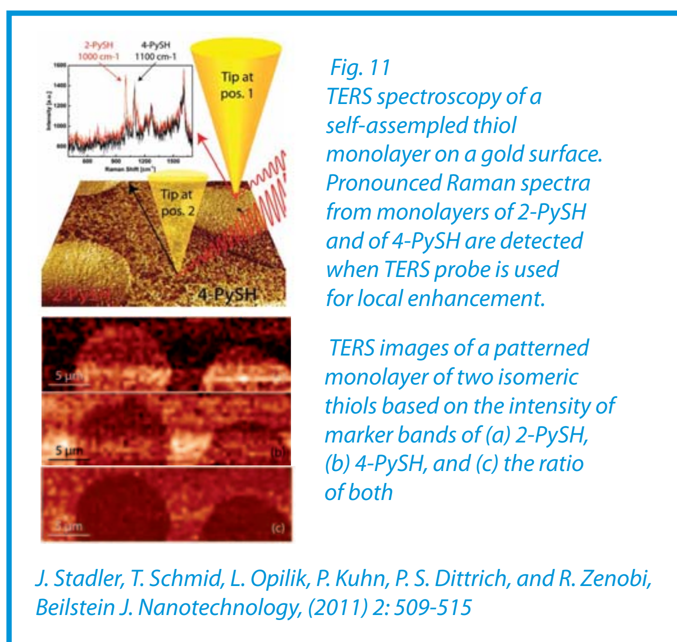

Fig. 11
TERS spectroscopy of a self-assempled thiol monolayer on a gold surface. Pronounced Raman spectra from monolayers of 2-PySH and of 4-PySH are detected when TERS probe is used for local enhancement.

TERS images of a patterned monolayer of two isomeric thiols based on the intensity of marker bands of (a) 2-PySH, (b) 4-PySH, and (c) the ratio of both

J. Stadler, T. Schmid, L. Opilik, P. Kuhn, P. S. Dittrich, and R. Zenobi, Beilstein J. Nanotechnology, (2011) 2: 509-515

TERS imaging of supported lipid layers

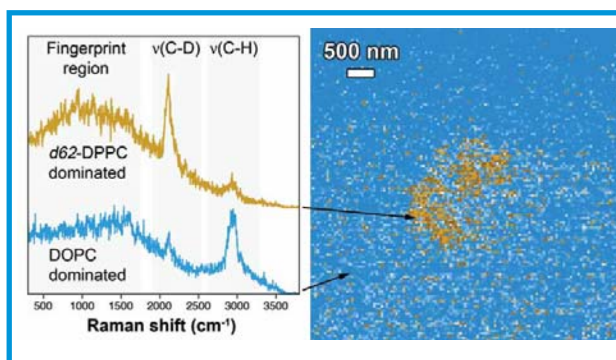

Fig. 12
STM-TERS allowed the direct measurement of the lipid distribution in a mixed supported lipid monolayer in a full-spectral map with high spatial resolution. The image is based on the intensity ratio of the C-D stretch mode (related to deuterated DPPC) and the C-H stretch mode (related to DOPC), and reveals an approx. 1-µm large domain that is dominated by DPPC. Supported lipid layers are model systems to gain insight into the processes associated with the compartmentalization of cell membranes into so-called lipid rafts.

AFM - Raman - SNOM - TERS
NTEGRA Spectra

Interdisciplinary Research at the Nanometer Scale

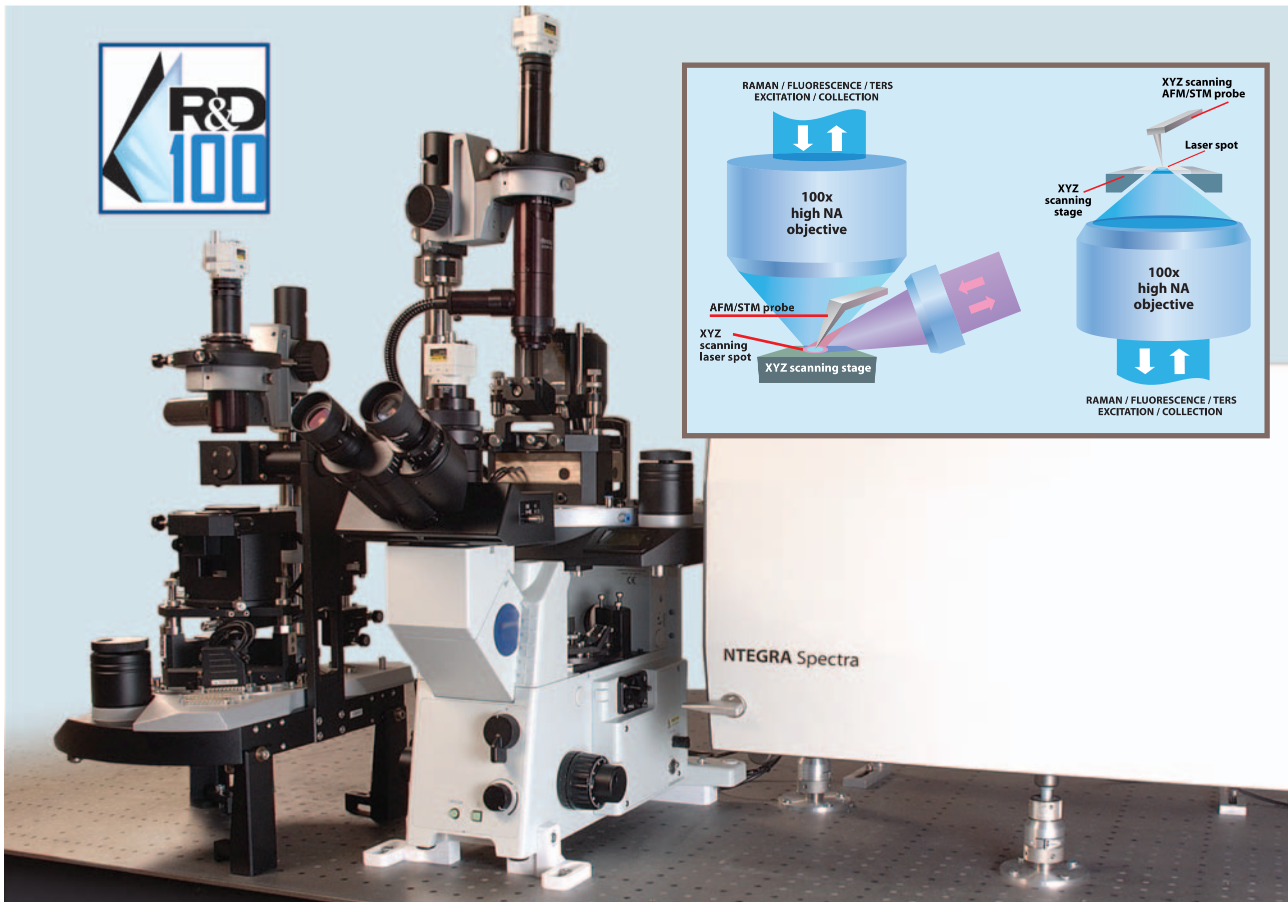

- Atomic Force Microscopy (>30 modes)
- Confocal Raman/fluorescence microscopy
- Optical microscopy
- Scanning near-field optical microscopy
- Tip-Enhanced Raman Scattering and other tip-assisted optical techniques (s-SNOM, TERM etc.)

Controlled Environment

Temperature – Humidity – Gases – Liquid – Electrochemical – Magnetic Field